JHEP

Published for SISSA by Springer

Received: *September 18, 2014*
Accepted: *October 9, 2014*
Published: *November 17, 2014*

Schrödinger functional boundary conditions and improvement for N > 3

Ari Hietanen,[a] **Tuomas Karavirta**[a] **and Pol Vilaseca**[b]

[a] *CP*^{3}*-Origins & the Danish IAS, University of Southern Denmark, Campusvej 55, Odense M, DK-5230 Denmark*

[b] *Instituto Nazionale di Fisica Nucleare, Sezione di Roma, P.le A. Moro 2, Roma, I-00185 Italia*

E-mail: hietanen@cp3-origins.net, karavirta@cp3-origins.net, pol.vilaseca.mainar@roma1.infn.it

Abstract: The standard method to calculate non-perturbatively the evolution of the running coupling of a SU(N) gauge theory is based on the Schrödinger functional (SF). In this paper we construct a family of boundary fields for general values of N which enter the standard definition of the SF coupling. We provide spatial boundary conditions for fermions in several representations which reduce the condition number of the squared Dirac operator. In addition, we calculate the $\mathcal{O}(a)$ improvement coefficients for $N > 3$ needed to remove boundary cutoff effects from the gauge action. After this, residual cutoff effects on the step scaling function are shown to be very small even when considering non-fundamental representations. We also calculate the ratio of Λ parameters between the $\overline{\text{MS}}$ and SF schemes.

Keywords: Lattice QCD, Lattice Gauge Field Theories, Lattice Quantum Field Theory

ArXiv ePrint: 1408.7047

doi:10.1007/JHEP11(2014)074

JHEP11(2014)074

Contents

JHEP11(2014)074

1 Introduction

Asymptotically free theories, such as gauge theories coupled to fermionic matter fields,[1] are characterized by having a coupling which becomes small at short distances. This property enables reliable perturbative calculations of physical quantities at large energies. A dimensionful scale is dynamically generated through the process of dimensional transmutation. Typically, this scale is associated in perturbation theory with the Λ parameter, i.e. a multiplicative constant of the integrated beta function.

The non-perturbative evolution of the running coupling in different gauge field theories from the low energy sector to the high energy regime has been the central goal of many studies. The standard approach is the use of a finite size scaling technique based on the Schrödinger functional (SF), in which the size of the system is associated to the renormalization scale [1]. This method was successfully used to calculate the scale evolution of the coupling in the SU(2) [2] and SU(3) [3] Yang-Mills theories and in QCD [4]. Motivated by ideas of physics beyond the standard model (BSM), in the last decade this method has

[1] For a small enough number of fermionic degrees of freedom.

also been applied to study the SU(4) pure gauge theory [5] and several theories containing matter transforming under higher dimensional representations of the gauge group or a large number of fermions in the fundamental representation [6–14].

However, for lattices accessible in typical numerical simulations SF schemes are affected by lattice artifacts arising from the bulk and from the boundaries of the lattice. These can be removed, following Symanzik's improvement program, by adding the corresponding counterterms to the action at the bulk and the boundaries. Symanzik's program was successfully carried out in [1, 15–18], where the improvement coefficients necessary to remove $O(a)$ effects from the coupling were calculated in perturbation theory.

For theories beyond QCD the situation is still inconclusive. A program for the non-perturbative study of SU(N) gauge theories in the large N limit [19] started in the last decade driven by interest from string theory. As part of that program, in [5] the ratio $\Lambda_{\overline{\rm MS}}/\sqrt{\sigma}$ between the lambda parameter in the $\overline{\rm MS}$ scheme and the string tension σ was calculated for the SU(4) theory aiming to obtain extrapolations of the N dependence of the $\Lambda_{\overline{\rm MS}}/\sqrt{\sigma}$ in the large N limit. There, the dominant systematic errors are due to the lattice artifacts present by using an unimproved action. For the case of theories with non-fundamental fermions, although the $O(a)$ improvement coefficients are known, the remaining higher order cutoff effects have been reported to be very large if the standard setups, which work fine for QCD, are naively exported.

In the last few years a new renormalized coupling based on the gradient flow (GF) has been proposed for step scaling studies [20–24]. Compared to the original SF coupling based on a background field (see bellow), the gradient flow coupling has the advantage that considerably smaller statistics are required for obtaining a similar accuracy.

However, there are some situations where the original SF coupling is superior compared to the gradient flow. First of all, it has been observed that while the GF coupling works better at large physical volumes, at small volumes the SF coupling fares better than the gradient flow [25]. Also, in the pure gauge theory, relevant for the large N limit, the generation of configurations is so fast compared to the measurement of the gradient flow that the reduced accuracy can be overcome with increased statistics. In addition, in BSM lattice studies one is often interested in the existence of a nontrivial infra-red fixed point. The value of the coupling constant g at the fixed point is a renormalization scheme dependent quantity and it differs between Schrödinger functional and gradient flow schemes. Therefore, it is possible that in a specific scheme the coupling is too strong at the fixed point or it is on the wrong side of a bulk phase transition. This is true even if the fixed point is visible in other schemes. The only study, we are aware of, that compares these two methods with the same action found the gradient flow coupling to be about twice the Schrödinger functional coupling [26]. Moreover, due to the property of continuum reduction [27], at large N it is possible to do simulations at small lattice volumes where the SF coupling is known to perform well.

This work completes the Schrödiger functional framework to study the phase diagram of strongly interacting gauge theories [28] with any N or representation. In the paper we generalize the boundary conditions for the gauge fields in the SF to obtain a family of schemes useful for arbitrary N with a good signal to noise ratio in lattice simulations.

JHEP11(2014)074

Moreover, the $O(a)$ improvement coefficients are obtained to one loop order in perturbation theory. For this, we calculate the one loop running coupling in our family of SF schemes following closely the discussions in [1, 15] and adapting them to arbitrary N. The values obtained for the boundary improvement coefficients are valid for any choice of Dirichlet boundary conditions at the temporal boundaries. With this knowledge we relate the Λ parameters between our SF schemes and the more widely used $\overline{\text{MS}}$ scheme. Another appealing property of the present family of schemes is that, together with an appropriate choice of spatial boundary conditions for the fermions, they lead to a setup for which higher order cutoff effects due to fermions are very small even for non-fundamental representations. Preliminary results of this work have been published in [29].

The paper is organized as follows: in section 2 we recall some concepts concerning the Schrödinger functional and collect a set of formulas useful for the remaining discussion. In section 3 the generalized boundary conditions are provided. The calculation of the improvement coefficients is presented in section 4, where we also discuss the effect that the fermionic spatial boundary conditions have on the residual higher order cutoff effects. The matching of the Λ parameters to the $\overline{\text{MS}}$ scheme is done in section 5. We conclude in section 6.

2 Schrödinger functional

In this section we briefly recall the ideas introduced in [1, 15, 30] and collect the expressions necessary for the subsequent discussion. We refer the interested reader to the original articles for further detail.

The Schrödinger functional is the euclidean propagation amplitude between a field configuration C at time 0 and another field configuration C' at time T, which has a path integral representation given by

$$\mathcal{Z}[C, C'] = \int \mathcal{D}[U, \bar{\psi}, \psi] e^{S[U,\bar{\psi},\psi]}, \tag{2.1}$$

with Dirichlet boundary conditions specified for the gauge fields U and the fermion fields ψ and $\bar{\psi}$.

In the present work, we are interested in the $\mathcal{O}(a)$ improved Wilson action

$$S[U, \bar{\psi}, \psi] = S_G[U] + S_F[U, \psi, \bar{\psi}]. \tag{2.2}$$

The pure gauge part is the standard SU(N) Wilson gauge action

$$S_G[U] = \frac{1}{g_0^2} \sum_P w(P) \text{Tr}[1 - \text{U(P)}]. \tag{2.3}$$

The spatial components of the gauge fields at the temporal boundaries ($t = 0$ and $t = T$) satisfy nonhomogeneous Dirichlet boundary conditions

$$U_k(t = 0, \boldsymbol{x}) = W_k(\boldsymbol{x}), \qquad U_k(t = T, \boldsymbol{x}) = W'_k(\boldsymbol{x}), \qquad k = 1, 2, 3. \tag{2.4}$$

JHEP11(2014)074

The boundary gauge fields W_k and W'_k can be parametrized as

$$W_k(\boldsymbol{x}) = \exp(aC_k(\eta)), \qquad W'_k(\boldsymbol{x}) = \exp(aC'_k(\eta)), \tag{2.5}$$

where $C_k(\eta)$ and $C'_k(\eta)$ are taken to be homogeneous, abelian and spatially constant [1], and they depend on a dimensionless parameter η. A specific form for these boundary matrices is derived in section 3 for gauge group SU(N) with arbitrary N. In the spatial directions the gauge fields are taken to be periodic $U_\mu(t, \boldsymbol{x}) = U_\mu(t, \boldsymbol{x} + L\hat{k})$.

The weight $w(P) = 1$ except for the spatial plaquettes at the boundaries for which $w(P) = \frac{1}{2}$. Due to the particular choice of boundary conditions for the gauge fields, the spatial boundary plaquettes give only a constant contribution to the action and can be ignored. It is well known that within SF schemes, the mere presence of temporal boundaries constitutes an extra source of lattice artifacts. Removal of these effects has first been studied in [1, 16, 17], where it was shown that the $\mathcal{O}(a)$ lattice artifacts coming from the boundaries can be canceled by tuning the weight $w(p) = c_t(g_0)$ for the temporal plaquettes attached to the boundaries, where c_t is the coefficient of a dimension 4 counterterm localized at the boundaries [1]. The perturbative expansion of c_t is

$$c_t = 1 + \left(c_t^{(1,0)} + c_t^{(1,1)} N_f\right) g_0^2 + \mathcal{O}(g_0^4), \tag{2.6}$$

where $c_t^{(1,0)}$ is the gauge and $c_t^{(1,1)}$ the fermionic contribution.

The fermionic part of eq. (2.2) is the standard Wilson fermion action with the clover term

$$S_F[U, \psi, \bar{\psi}] = a^4 \sum_x \bar{\psi}(x)(D_{\mathrm{WD}} + m_0)\psi(x), \tag{2.7}$$

where D_{WD} is the improved Wilson-Dirac operator

$$D_{\mathrm{WD}} = \frac{1}{2}[\gamma_\mu(D^*_\mu + D_\mu) - aD^*_\mu D_\mu] + c_{\mathrm{sw}} \frac{ia}{4} \sigma_{\mu\nu} F_{\mu\nu}(x). \tag{2.8}$$

The operator $F_{\mu\nu}(x)$ is the symmetrized lattice field strength tensor, $\sigma_{\mu\nu} = \frac{i}{2}[\gamma_\mu, \gamma_\nu]$ and the operators D_μ and D^*_μ are the covariant forward and backward derivatives which are defined in eq. (A.8). The improvement coefficient c_{sw} can be determined perturbatively [16, 31] and non-perturbatively [32, 33]. To the lowest order in perturbation theory $c_{\mathrm{sw}} = 1$ [18]. The removal of $O(a)$ effects arising from the interplay between fermions and the SF boundaries requires the addition of another dimension 4 counterterm at the boundaries. Since this does not contribute to the observables studied further in this work at the present order in perturbation theory, we ignore it from now on and refer the reader to the original literature [17] for further details.

The fermionic fields satisfy the following boundary conditions

$$P_+\psi|_{t=0} = P_-\psi|_{t=T} = 0, \tag{2.9}$$

$$\bar{\psi}P_-\big|_{t=0} = \bar{\psi}P_+\big|_{t=T} = 0, \tag{2.10}$$

where $P_\pm = \frac{1}{2}(1 \pm \gamma_0)$. The boundary conditions in the spatial directions are periodic up to a phase [30]:

$$\psi(x + L\hat{k}) = e^{i\theta_k}\psi(x), \qquad \bar{\psi}(x + L\hat{k}) = \bar{\psi}(x)e^{-i\theta_k}. \tag{2.11}$$

JHEP11(2014)074

The phase is usually chosen so that the smallest eigenvalue of the squared Dirac operator is large [30]. In this situation, the condition number (i.e. the ratio between the highest an lowest eigenvalues) is small, which improves the speed of the known inversion algorithms. However, the value of θ also has an effect on the convergence of the 1-loop perturbative coupling to its continuum limit. This is discussed in subsection 4.3.

The boundary conditions for the gauge fields in eqs. (2.4) and (2.5) induce a constant chromo-electric background field $V_\mu(x)$ in the space-time. The variable η in the boundary fields eq. (2.5) parametrizes a curve of background fields. A renormalized coupling can be defined [1] as a response of the system to a deformation of the background field

$$\left.\frac{\partial\Gamma}{\partial\eta}\right|_{\eta=0} = \frac{\kappa}{\overline{g}^2}, \tag{2.12}$$

with the effective action $\Gamma = -\ln\mathcal{Z}$. The normalization constant

$$\kappa = \left.\frac{\partial\Gamma_0}{\partial\eta}\right|_{\eta=0}, \tag{2.13}$$

is defined so that $\overline{g}^2 = g_0^2$ to the lowest order of perturbation theory.

One of the central quantities in numerical simulations is the step scaling function

$$\sigma(u) = \overline{g}^2(2L)\big|_{u=\overline{g}^2(L)}\,. \tag{2.14}$$

This is required for reconstructing non-perturbatively the scale evolution of the running coupling. In presence of a lattice regulator, the deviations of the lattice counterpart of the step scaling function $\Sigma(u, L/a)$ from the continuum $\sigma(u)$ can be used to monitor the size of cutoff effects (see subsection 4.3).

2.1 1-loop expansion

The renormalized coupling eq. (2.12) is suitable for both perturbative and non-perturbative evaluation. The 1-loop calculation of eq. (2.12) was done in [1, 3] for the pure gauge theory in SU(2), and extended to accommodate fermions in [30].[2] Non fundamental fermions have been considered in [34–36]. In the present work we extend the previous calculations to arbitrary N. Although the main strategy of the calculation follows closely previous works, some care has to be taken to generalize those ideas without complicating the calculation. In the present subsection we collect some formulas necessary for the subsequent discussion and leave all technical details on the calculation to appendices A and B.

After going through the gauge fixing procedure [1], the effective action is expanded to 1-loop as

$$\Gamma = g_0^{-2}\Gamma_0 + \Gamma_1 + \mathcal{O}(g_0^2). \tag{2.15}$$

Here Γ_0 is the classical action. The 1-loop term Γ_1 in the effective action can be written as

$$\Gamma_1 = -\ln\det\Delta_0 + 1/2\ln\det\Delta_1 - 1/2\ln\det\Delta_2, \tag{2.16}$$

[2]The evaluation of eq. (2.12) to 2 loops was done in [37, 38].

JHEP11(2014)074

where Δ_0, Δ_1 and Δ_2 are the quadratic ghost, gluonic and fermionic operators respectively. The explicit forms of the operators Δ_i are given in appendix A.

The renormalized coupling eq. (2.12) is also expanded in perturbation theory

$$\bar{g}^2(L/a) = g_0^2 + p_1(L/a)g_0^4 + \mathcal{O}(g_0^6). \tag{2.17}$$

According to eq. (2.15), the 1-loop coefficient

$$p_1(L/a) = -\frac{\partial\Gamma_1/\partial\eta}{\partial\Gamma_0/\partial\eta}, \tag{2.18}$$

receives an independent contribution from ghost, gauge, and fermionic fields

$$p_1(L/a) = h_0(L/a) - \frac{1}{2}h_1(L/a) + \frac{1}{2}h_2(L/a) = p_{1,0}(L/a) + N_f p_{1,1}(L/a), \tag{2.19}$$

with

$$h_s = \frac{1}{\kappa}\frac{\partial}{\partial\eta}\ln(\det\Delta_s), \qquad s = 0, 1, 2. \tag{2.20}$$

The gauge and fermionic contributions to eq. (2.19) can be calculated independently. The gauge part is given by

$$p_{1,0}(L/a) = h_0(L/a) - \frac{1}{2}h_1(L/a). \tag{2.21}$$

The calculation of $h_0(L/a)$ and $h_1(L/a)$ has been described in great detail for SU(2) in [1] and the calculation has been done for $N = 3$ in [3]. In appendix A we give the generalization of the calculations to $N \geq 3$.

The calculation of the fermionic part $p_{1,1}(L/a)$ is straight forward to generalize to any boundary fields and to any representation of the gauge group. One just needs to replace the link variables in the Wilson Dirac operator eq. (2.8) with their counterparts in the desired representation. Thus we will refer the interested reader to the original paper [15].

The continuum and lattice step scaling functions are given to first order in perturbation theory by

$$\sigma(u) = u + \sigma_1 u^2 + \mathcal{O}(u^3), \qquad \Sigma(L/a, u) = u + \Sigma_1(L/a)u^2 + \mathcal{O}(u^3), \tag{2.22}$$

with $\sigma_1 = 2b_0\ln(2)$. The 1-loop coefficient b_0 of the beta function is given in an arbitrary representation by

$$b_0 = b_{0,0} + N_f b_{0,1}, \qquad b_{0,0} = \frac{1}{(4\pi)^2}\frac{11}{3}C_2(F), \qquad b_{0,1} = -\frac{1}{(4\pi)^2}\frac{4}{3}T_R, \tag{2.23}$$

where the color group invariants are defined as

$$C_2(A)\delta^{AB} = f^{ACD}f^{BCD}, \qquad T_R\delta^{AB} = \mathrm{Tr}[t^A t^B], \qquad C_2(R) = t^A t^A, \tag{2.24}$$

in the representation R of SU(N).[3]

[3]The values of the invariants are given by $T_F = 1/2$, $C_2(F) = N$, $T_A = N$, $C_2(A) = (N^2-1)/(2N)$, $T_S = (N+2)/2$, $C_2(S) = (N-1)(N+2)/N$, $T_{AS} = (N-2)/2$ and $C_2(AS) = (N+1)(N-2)/N$ for the fundamental, adjoint, symmetric and antisymmetric representations respectively.

JHEP11(2014)074

Similarly as in eq. (2.19), the step scaling functions can be separated into a gauge and a fermionic part,

$$\sigma_1 = \sigma_{1,0} + N_f\sigma_{1,1}, \qquad \Sigma_1(L/a) = \Sigma_{1,0}(L/a) + N_f\Sigma_{1,1}(L/a). \tag{2.25}$$

This allows us to study separately cutoff effects due to gauge and fermion fields independently.

3 Boundary fields for $N > 2$

In this section we present a generalization of the boundary fields for $N > 2$. The selection of the boundary fields is only limited by the requirement that there is a unique and stable classical solution to system. In practice, this limits us to Abelian boundary fields W_k and W'_k which can be written as in eq. (2.5), where

$$C_k = \frac{i}{L}\begin{pmatrix} \phi_1 & 0 & \dots & 0 \\ 0 & \phi_2 & \dots & 0 \\ \vdots & \vdots & \ddots & \vdots \\ 0 & 0 & \dots & \phi_N \end{pmatrix} \qquad \text{and} \qquad C'_k = \frac{i}{L}\begin{pmatrix} \phi'_1 & 0 & \dots & 0 \\ 0 & \phi'_2 & \dots & 0 \\ \vdots & \vdots & \ddots & \vdots \\ 0 & 0 & \dots & \phi'_N \end{pmatrix}. \tag{3.1}$$

Since W_k has to be an SU(N)-matrix the vectors $\boldsymbol{\phi} = (\phi_1, \phi_2, \dots, \phi_N)$ and $\boldsymbol{\phi}' = (\phi'_1, \phi'_2, \dots, \phi'_N)$ must satisfy

$$\sum_{k=1}^{N} \phi_k = 0. \tag{3.2}$$

Now the classical solution, i.e. the background field, can be written as

$$V_\mu(x) = \exp(aB_\mu(x)), \tag{3.3}$$

where

$$B_0(x) = 0, \tag{3.4}$$

$$B_k(x) = [x^0 C'_k + (L - x^0)C_k]/L. \tag{3.5}$$

It is shown in [1] that the solution $V_\mu(x)$ is absolutely stable if the vectors $\boldsymbol{\phi}$ and $\boldsymbol{\phi}'$ satisfy eq. (3.2) and

$$\phi_1 < \phi_2 < \ldots < \phi_N, \tag{3.6}$$

$$\phi_N - \phi_1 < 2\pi. \tag{3.7}$$

These conditions define a fundamental domain, which is an irregular $(N-1)$-simplex and has vertices at points

$$\boldsymbol{X}_1 = \frac{2\pi}{N}\left(-N+1, 1, 1, \dots, 1\right), \tag{3.8}$$

$$\boldsymbol{X}_2 = \frac{2\pi}{N}\left(-N+2, -N+2, 2, \dots, 2\right), \tag{3.9}$$

$$\boldsymbol{X}_3 = \frac{2\pi}{N}\left(-N+3,-N+3,-N+3,3,\ldots,3,\right), \tag{3.10}$$

$$\vdots \tag{3.11}$$

$$\boldsymbol{X}_{N-1} = \frac{2\pi}{N}\left(-1,-1,\ldots,-1,N-1\right), \tag{3.12}$$

$$\boldsymbol{X}_N = (0,0,\ldots,0). \tag{3.13}$$

To define a renormalized coupling we can choose any two different points inside the fundamental domain to set up the boundary fields. A different choice leads to a different renormalization scheme, which can be matched to each other using perturbation theory (see section 5). However, there are practical considerations in selecting the boundary fields, namely the signal to noise ratio in the Monte Carlo simulations and the size of higher order lattice artifacts. Our choice is based on the attempt to maximize the signal to noise ratio as in practice the minimization of the higher order lattice artifacts often leads to a low signal, which neglects the gains of a better continuum extrapolation.

To obtain a maximal signal strength we have two competing requirements. We need to twist the gauge fields as much as possible while staying away from the boundaries of the fundamental domain. This is because the coupling is proportional to the twist and because closeness of the instability of the classical solution increases noise. According to these considerations we choose ϕ to be in the middle of a line connecting $\boldsymbol{X}_1$ and the centeroid of the fundamental domain

$$\begin{aligned}\boldsymbol{\phi} &= \frac{1}{2}\boldsymbol{X_1} + \frac{1}{2N}\sum_{k=1}^{N}\boldsymbol{X}_k \\ &= \frac{\pi}{2N}\left(3-3N,5-N,7-N,\ldots,N+1\right).\end{aligned} \tag{3.14}$$

To determine $\boldsymbol{\phi}'$ we find a transformation which is a map from the fundamental domain to itself and mirrors the vertices. First we define a simple map $R_{i,j}(\boldsymbol{\phi})$ that reflects the points in the fundamental domain with respect to a $(N-2)$ dimensional hyperplane. The hyperplane $R_{i,j}(\boldsymbol{\phi})$ goes through vertices $\boldsymbol{X}_k$, $k \neq i,j$ and intersects the line connecting $\boldsymbol{X}_i$ and $\boldsymbol{X}_j$ at the middle. For $N > 3$ the function $R_{i,j}(\boldsymbol{\phi})$ is not in general a mapping from the fundamental domain to itself, but we can define a composite mapping

$$\mathcal{M}(\boldsymbol{\phi}) = \left(R_{1,N-1} \circ R_{2,N-2} \circ \ldots \circ R_{[N/2],N-[N/2]}\right)(\boldsymbol{\phi}), \tag{3.15}$$

where $R_{i,i}(\boldsymbol{\phi})$ is the identity mapping and $[x]$ denotes the integer part of x. Now $\mathcal{M}(\boldsymbol{\phi})$ is a mapping from the fundamental domain to itself and written in components it has a simple form

$$\phi'_i = \left[\mathcal{M}(\boldsymbol{\phi})\right]_i = -\phi_{N-i+1}. \tag{3.16}$$

To define the coupling we choose a one parameter curve of background fields $\boldsymbol{\phi} + \boldsymbol{t}(\eta)$. We select it in a way that the results are equivalent to those of the SU(3) theory given in [3],[4] i.e. we select $\boldsymbol{t}(\eta)$ so that it changes sign under the mapping $\mathcal{M}(\phi)$ and points

[4]Note that the boundaries are trivially rotated compared to the ones in [3].

JHEP11(2014)074

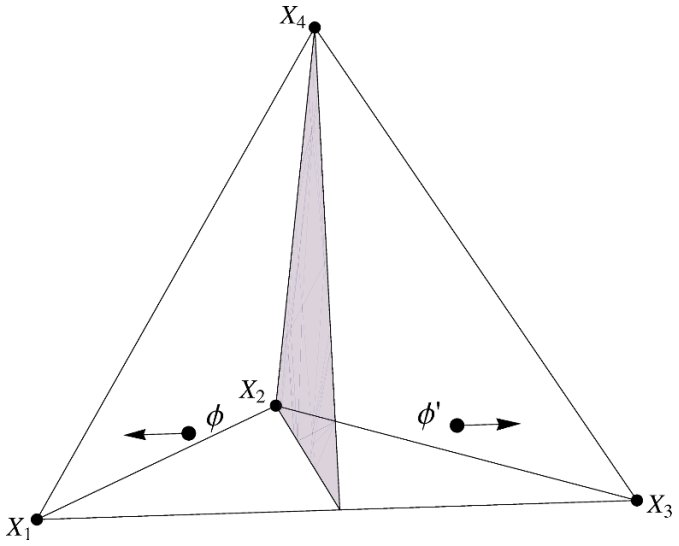

Figure 1. Fundamental domain of SU(4).

towards the boundaries of the fundamental domain

$$\begin{aligned} \boldsymbol{t}(\eta) &= \frac{\eta N}{2\pi(N-2)} \left(\boldsymbol{X}_1 - \boldsymbol{X}_{N-1}\right) \\ &= \left(-\eta, \frac{2\eta}{N-2}, \ldots, \frac{2\eta}{N-2}, -\eta\right). \end{aligned} \tag{3.17}$$

See figure 1 for illustration of the fundamental domain and boundary conditions for SU(4) and table 1 for the boundary values for $N = 3, 4, 5$.

In the lattice computations it is advisable *not* to set $\boldsymbol{t}(\eta)$ beforehand, but to measure a complete $N-1$ dimensional basis which can be used to construct a generic curve. Each curve corresponds to a different renormalization scheme.

4 Boundary effects and improvements

4.1 Fermionic spatial boundary conditions

Recalling the spatial boundary conditions for the fermion fields eq. (2.11), we still have to choose a particular value for the angles θ_k. For simplicity, we consider the same angle in all spatial directions $\theta = \theta_k$, $k = 1, 2, 3$.

We then fix θ, following the criteria introduced in [15], so that the minimum eigenvalue λ_{min} of the fermion operator Δ_2 is as large as possible. This leads to a small condition number which optimizes the speed of the numerical inversion of the operator.

The values of θ leading to a maximum λ_{min} depend on the background field and also on the fermion representation being considered. For the fundamental representation, the profile of smallest eigenvalues λ_{min} as a function of θ is shown in figure 2 for the different gauge groups considered in this work excluding the case of SU(2).

Although the maximum of λ_{min} is achieved at different values of θ for every gauge group considered, the choice $\theta = \pi/2$ is always close to the maximum and hence leads to

JHEP11(2014)074

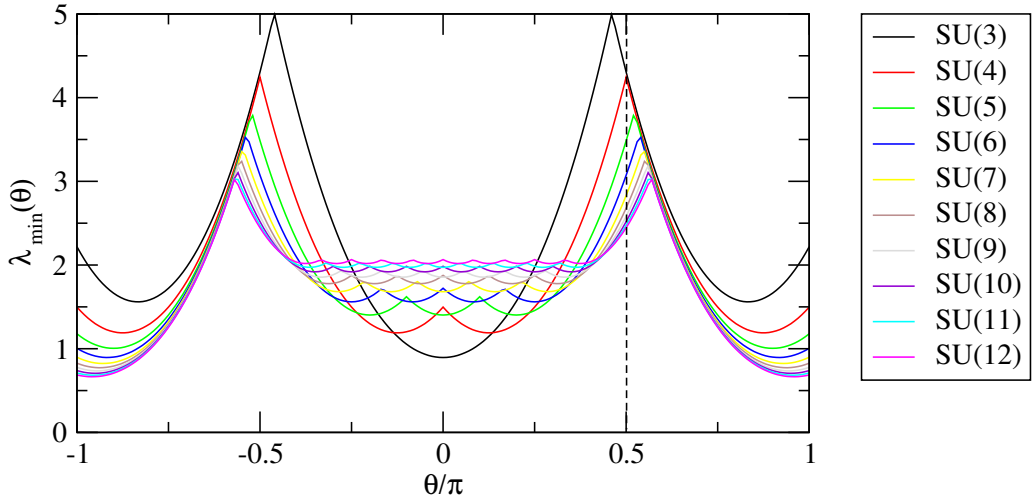

Figure 2. Lowest eigenvalue $\lambda_{\min}$ (in units of L^{-2}) as a function of θ for the fundamental representation of SU(N), with $N \subset [3, 12]$. The vertical discontinuous line marks the chosen value $\theta = \pi/2$.

$N = 3$	
ϕ	ϕ'
$-\eta - \pi$	$\eta - \frac{2\pi}{3}$
$2\eta + \frac{\pi}{3}$	$-2\eta - \frac{\pi}{3}$
$-\eta + \frac{2\pi}{3}$	$\eta + \pi$

$N = 4$	
ϕ	ϕ'
$-\eta - \frac{9}{8}\pi$	$\eta - \frac{5}{8}\pi$
$\eta + \frac{1}{8}\pi$	$-\eta - \frac{3}{8}\pi$
$\eta + \frac{3}{8}\pi$	$-\eta - \frac{1}{8}\pi$
$-\eta + \frac{5}{8}\pi$	$\eta + \frac{9}{8}\pi$

$N = 5$	
ϕ	ϕ'
$-\eta - \frac{6}{5}\pi$	$\eta - \frac{3}{5}\pi$
$\frac{2}{3}\eta$	$-\frac{2}{3}\eta - \frac{2}{5}\pi$
$\frac{2}{3}\eta + \frac{1}{5}\pi$	$-\frac{2}{3}\eta - \frac{1}{5}\pi$
$\frac{2}{3}\eta + \frac{2}{5}\pi$	$-\frac{2}{3}\eta$
$-\eta + \frac{3}{5}\pi$	$\eta + \frac{6}{5}\pi$

Table 1. The values of the boundary fields for $N = 3, 4, 5$.

a small condition number. For homogeneity in the definition of a renormalization scheme in the subsequent calculations, we will fix $\theta = \pi/2$ for all values of N. As we will show in subsection 4.3, this choice of θ together with the family of background fields defined in this work will lead to a setup for which higher order cutoff effects are highly suppressed even for non-fundamental representations. Although the choice of $\theta = \pi/2$ is taken considering the fundamental representation, this value also leads to reasonably small condition numbers for the symmetric and antisymmetric representations. For the adjoint representation the smallest condition number is obtained for $\theta = 0$. However, we decide to stick to the choice $\theta = \pi/2$ also in this case since it leads to a situation were higher order lattice artifacts are highly reduced.[5]

For the case of SU(2), we choose $\theta = 0$ for the fundamental representation but leave $\theta = \pi/2$ for the symmetric/adjoint.

[5]We consider the reduction of higher order cutoff effects, which have been shown to be very large [34–36], to be of higher importance.

JHEP11(2014)074

4.2 Gauge boundary improvement

4.2.1 Expansion

The variables $p_{1,i}(L/a)$ are expected to have an asymptotic expansion in L/a [1]

$$p_{1,i}(L/a) \sim \sum_{n=0}^{\infty} (r_{n,i} + s_{n,i} \ln(L/a)) \left(\frac{a}{L}\right)^n , \tag{4.1}$$

where $s_{0,i} = 2b_{0,i}$ and $s_{1,i} = 0$ after setting $c_{\rm sw}$ to its tree level value. The boundary improvement coefficients $c_t^{(1,i)}$ are determined by demanding linear cutoff effects to be absent in eq. (4.1), which is achieved by fixing $c_t^{(1,i)} = r_{1,i}/2$. The continuum coefficients $r_{0,i}$ are needed when matching the Λ parameter to other schemes.

In order to extract the coefficients $r_{n,i}$ as accurately as possible we first evaluate $p_{1,0}(L/a)$ and $p_{1,1}(L/a)$ adapting the strategies in [1, 15] to general N (see appendices A and B for details on the calculation). Once the series of data for $p_{1,i}(L/a)$ is produced, the coefficients $r_{n,i}$ can be extracted using a suitable fitting procedure.

In the pure gauge case, we calculated $p_{1,0}(L/a)$ for values of $L/a \in \{6, 8, \ldots, 100\}$ and then used the "Blocking" method described in [39] to obtain the values of the asymptotic coefficients. The calculation was done using floating point precision with 50 decimal places for $2 \leq N \leq 8$ and with quadruple precision for $N > 8$. To control the error we compared the results and errors obtained with different level of accuracy. Since the asymptotic form eq. (4.1) is expected to be valid as $a/L \to 0$, we consider only values of $L/a \subset [28, 100]$ when extracting the coefficients $r_{0,0}$ and $r_{0,1}$. This choice produced the most reliable values for the coefficients and their relative errors. As a check we also reproduced the known value of $s_{0,0} = 2b_{1,0}$ to a similar degree of accuracy.

Concerning the fermionic part, values for $p_{1,1}(L/a)$ were produced at quadruple precision in the range $L/a \subset [4, 64]$ (for even and odd values) for all gauge groups and representations considered in this work. This was enough to obtain the asymptotic coefficients in eq. (4.1) to very high precision (see tables 2 and 3).

4.2.2 Results

In table 2 we give the values for the coefficients $r_{0,0}$ and $r_{1,0}$. From $r_{1,0}$ we can extract the gauge contribution to the boundary improvement coefficient $c_t^{(1,0)} = \frac{1}{2} r_{1,0}$. According to continuum perturbation theory we expect $c_t^{(1,0)}$ to depend on group theoretical factors with the functional form

$$c_t^{(1,0)} = AC_2(F) + BC_2(A) \equiv aN + \frac{b}{N}, \tag{4.2}$$

where $C_2(R)$ is the quadratic Casimir operator in the representation R. A fit to the data gives $b = 0.017852(13)$ and $a = -0.0316483(4)$ with an excellent $\chi^2/\text{d.o.f.} \approx 2.2/9 \approx 0.24$. The data and the fit are shown in figure 3. To check the consistency of our results, we have also performed fits adding additional terms to eq. (4.2). The coefficients of the additional terms are zero within statistical errors as shown in table 4.

JHEP11(2014)074

N	$r_{0,0}$	$r_{1,0}$
2	0.202349528(3)	-0.108735(17)
3	0.368282146(3)	-0.177987(14)
4	0.520970830(2)	-0.244261(14)
5	0.673474985(2)	-0.309345(13)
6	0.826895868(3)	-0.373834(13)
7	0.981591358(3)	-0.437984(13)
8	1.137655320(3)	-0.501921(12)
9	1.295080018(5)	-0.565696(18)
10	1.45381790(5)	-0.629390(18)
11	1.61380703(5)	-0.693011(14)
12	1.77498215(5)	-0.756579(14)

Table 2. Values of the pure gauge coefficients $r_{0,0}$ and $r_{1,0}$ for $N = 2, \ldots, 12$.

N	Fundamental	Adjoint	Symmetric	Antisymmetric
2	-0.00342666(1)	-0.13787329(4)	-0.13787329(4)	-
3	-0.00343842(1)	-0.20761772(4)	-0.17327682(5)	-0.00343842(1)
4	-0.00344138(2)	-0.27682313(6)	-0.20788611(5)	-0.06893677(2)
5	-0.00344277(1)	-0.34620010(5)	-0.24257541(4)	-0.10364831(4)
6	-0.00344355(1)	-0.41563817(4)	-0.27729937(5)	-0.13840671(4)
7	-0.00344406(1)	-0.48510052(4)	-0.31204105(4)	-0.17317365(5)
8	-0.00344441(1)	-0.55457355(5)	-0.34679040(5)	-0.20793990(4)
9	-0.00344468(1)	-0.62405117(5)	-0.38154235(4)	-0.24270438(2)
10	-0.00344489(1)	-0.69353094(5)	-0.41629290(6)	-0.27746570(5)
11	-0.00344506(1)	-0.76295832(5)	-0.45104376(5)	-0.31122243(3)
12	-0.00344520(1)	-0.83249201(5)	-0.48579212(5)	-0.34698044(4)

Table 3. Values of the fermionic coefficient $r_{0,1}$ for the fundamental, adjoint, symmetric and antisymmetric representations of $N = 2, \ldots, 12$.

For completeness, we also include here the value of the fermionic part $c_t^{(1,1)}$ for an arbitrary group and representation

$$c_t^{(1,1)}(R) = 0.038282(2)T_R. \tag{4.3}$$

This was calculated for the fundamental representation in [15] and later extended to other represesentations in [35]. In the present work we have been able to reproduce the value of $c_t^{(1,1)}$ with similar accuracy, which is a further check on the correctness of the whole calculation.

4.3 Residual cutoff effects

The determination of the gauge and fermion contributions to $c_t^{(1)}$ removes $O(a)$ lattice artifacts coming from the boundaries to 1-loop in perturbation theory. However, cutoff effects of higher order in a are still present. We quantify these using the relative deviations

JHEP11(2014)074

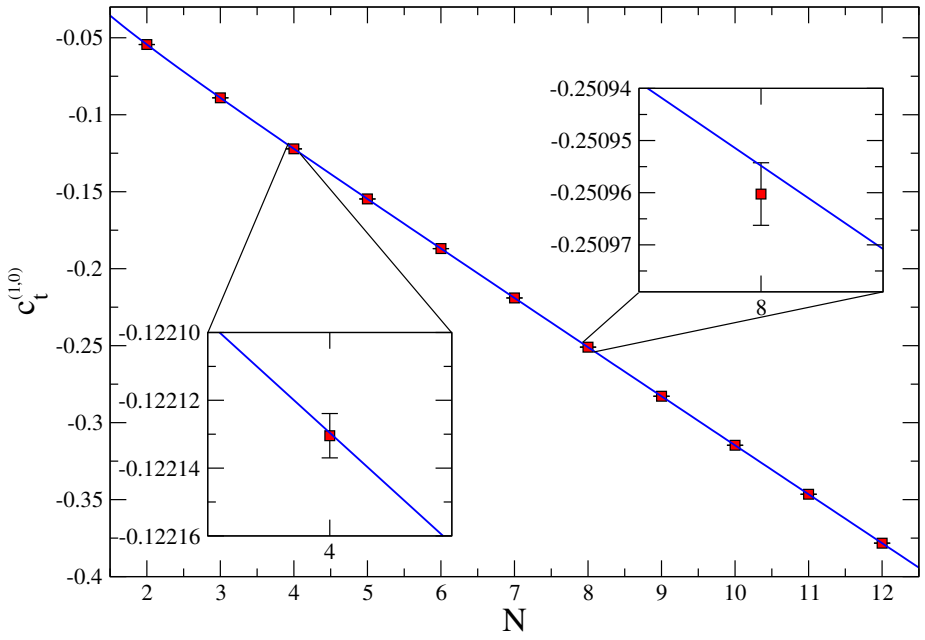

Figure 3. A polynomial fit to the $c_t^{(1,0)}$ data. We have zoomed out two points to illustrate the accuracy of the fit.

Fit function	Parameters	χ^2/d.o.f.
$aN + b/N$	$a = -0.0316483(4)$ $b = 0.017852(13)$	2.2/9=0.24
$aN + b + c/N$	$a = -0.0316469(14)$ $b = -1.7(16) \times 10^{-5}$ $c = 0.01789(4)$	1.0/8=0.13
$aN^2 + bN + c + d/N + e/N^2$	$a = -2(135) \times 10^{-8}$ $b = -0.03164(4)$ $c = -5(26) \times 10^{-5}$ $d = 0.0180(9)$ $e = -2(8) \times 10^{-5}$	0.76/6=0.13

Table 4. Fits with a different functional forms for $c_t^{(1,0)}$.

from the pure gauge and pure fermionic lattice step scaling functions to one loop order, with respect to their universal continuum counterparts

$$\delta_{1,i}(a, L) = \frac{\Sigma_{1,i}(L/a) - \sigma_{1,i}}{\sigma_{1,i}}, \qquad \Sigma_{1,i}(L/a) = p_{1,i}(2L/a) - p_{1,i}(L/a). \tag{4.4}$$

In figure 4 we show the convergence of the gauge part of the 1-loop step scaling function with and without improvement. It can be seen immediately that the residual cutoff effects

JHEP11(2014)074

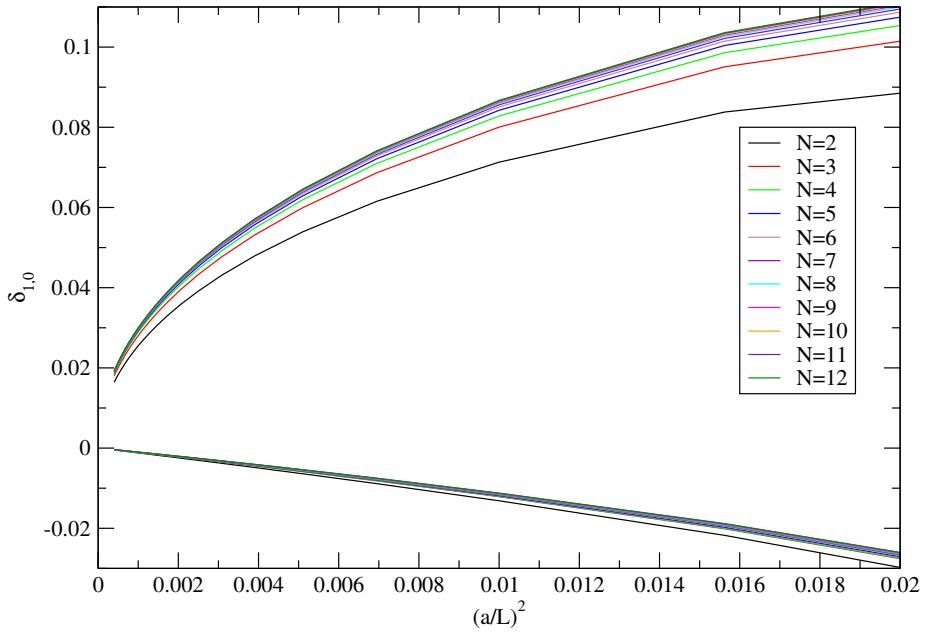

Figure 4. Cutoff effects in the gauge part of the 1-loop step scaling function with $c_t^{(1,0)} = 0$ (upper set of lines) and with $c_t^{(1,0)}$ set to its perturbative value (lower set of lines).

after improvement are quadratic in (a/L) and small (order of 1%) at $L/a = 10$. Also the result depends only mildly on N.

The cutoff effects due to fundamental fermions are displayed in panel (a) of figure 5. From there, it is clear that in all the gauge groups considered in this work, the residual higher order cutoff effects are rather small after boundary $O(a)$ improvement is implemented. Residual cutoff effects are of the order of 10% already at the coarsest lattices considered, and converge to zero very fast.

This is true for the family of background fields defined in section 3 and for the value of θ chosen in subsection 4.1. A different choice of parameters, however, can lead to very high residual cutoff effects even after boundary $O(a)$ improvement is implemented.[6] In order to check this, we study the dependence of $\delta_{1,1}$ on the parameter θ for different values of N in a range $\theta \subset [0.45\pi, 0.57\pi]$. The cases of $N = 3$ and 6 are displayed in figure 6. Other gauge groups show a very similar behavior. The residual cutoff effects $\delta_{1,1}$ depend strongly on θ. Clearly, a poor choice of θ might lead to situations with very large higher order cutoff effects.[7]

It is remarkable that the value $\theta = \pi/2$, established in subsection 4.1 to obtain a condition number as small as possible, also leads to a situation where higher order cutoff effects are highly suppressed.

A very similar picture is observed when considering any of the 2-index representations. Cutoff effects for the adjoint, symmetric and anti-symmetric representations are shown

[6] See references [34–36] for this issue in representations other than the fundamental.

[7] Note that the value $\theta = \pi/5$ chosen in [15] leads to very reduced cutoff effects for their choice of BF. This would not be the case if this value was used with our BF.

JHEP11(2014)074

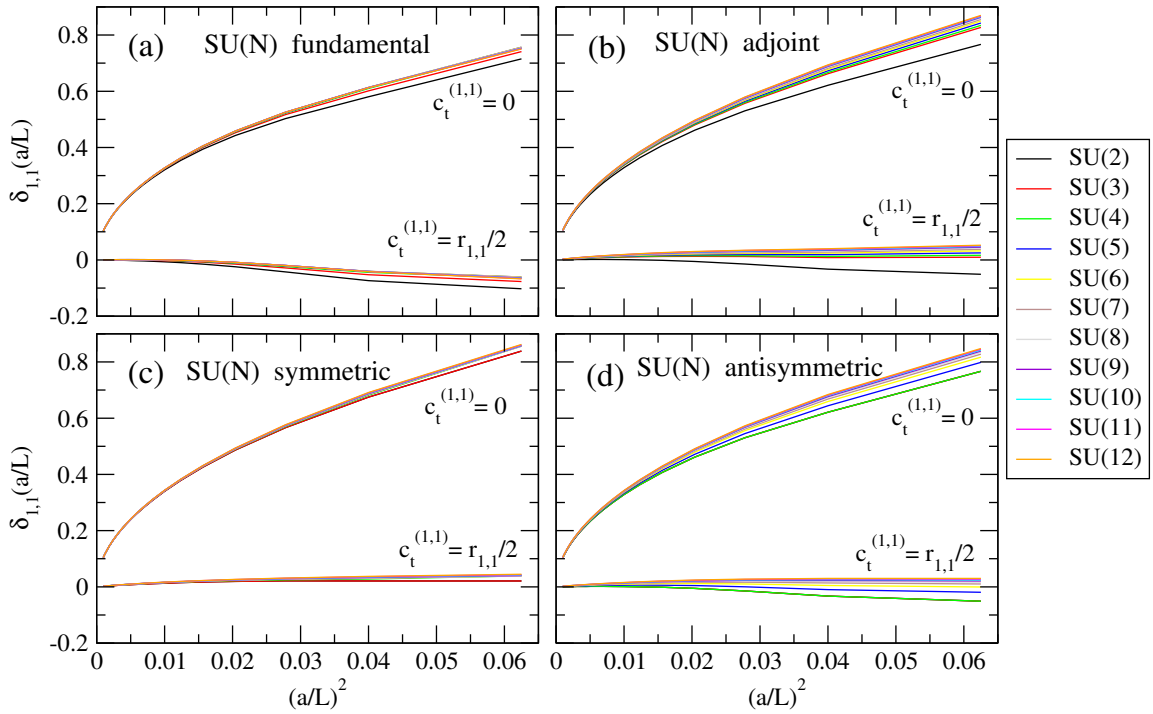

Figure 5. Cutoff effects in the fermionic part of the 1-loop step scaling function due to a single flavor in the fundamental (a), adjoint (b), symmetric (c) and antisymmetric (d) representations for the gauge groups considered in this work. Cutoff effects are shown before ($c_t^{(1,1)} = 0$) and after ($c_t^{(1,1)} = r_{1,1}/2$) implementing $O(a)$ boundary improvement.

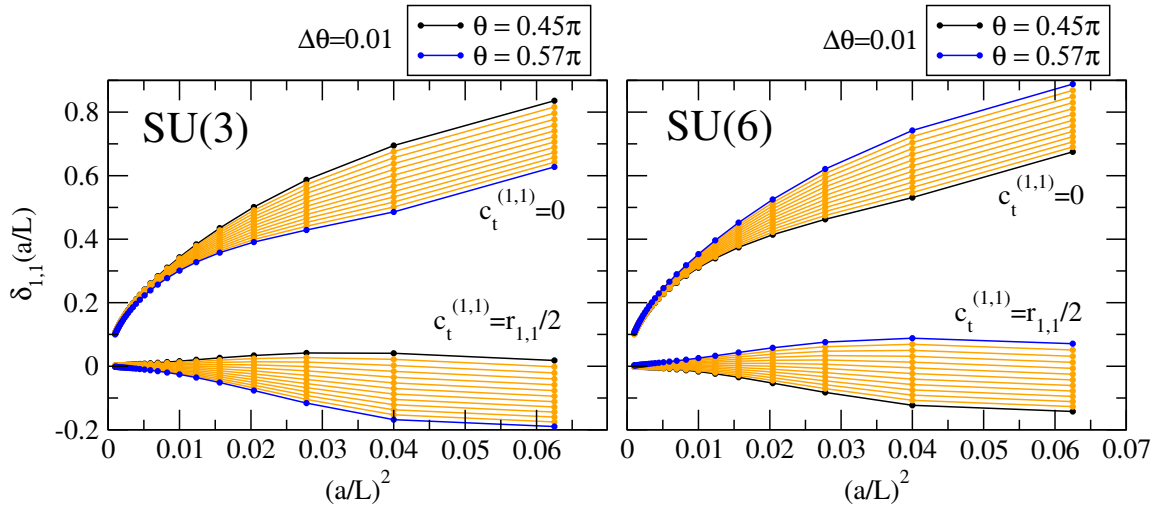

Figure 6. Cutoff effects in the fermionic part of the 1-loop step scaling function for $N = 3$ and 6. Cutoff effects are shown before ($c_t^{(1,1)} = 0$) and after ($c_t^{(1,1)} = r_{1,1}/2$) implementing $O(a)$ boundary improvement.

respectively in panels (b), (c) and (d) of figure 5. The smallness of the residual lattice artifacts is at first glance surprising, since they have previously been reported to be very

JHEP11(2014)074

large if particular care is not taken in the choice of BF [34–36]. The magnitude of $\delta_{1,1}$ for the 2-index representations strongly depends on the angle θ in a very similar way as it is shown in figure 6 for the fundamental representation. It is then possible to tune θ to minimize cutoff effects without the need of modifying the BF [35, 36]. What is remarkable of the family of background fields proposed in this work is that for the fundamental, symmetric and antisymmetric representations, values of θ which lead to small condition numbers also lead to small higher order lattice artifacts in the step scaling function. This is not true for the adjoint representation since, as discussed in subsection 4.1, the condition number is minimized for $\theta = 0$. It is also remarkable that cutoff effects for all the representations considered are minimized for the same value $\theta = \pi/2$.

5 Matching the Λ parameter to $\overline{\text{MS}}$

In this section we calculate the relation $\Lambda_{\text{SF}}/\Lambda_{\overline{\text{MS}}}$ of Λ parameters in our family of SF schemes and the $\overline{\text{MS}}$ scheme. This relation is essential for obtaining the ratio $\Lambda_{\overline{\text{MS}}}/\sqrt{\sigma}$ from SF simulations. We provide numerical values of $\Lambda_{\text{SF}}/\Lambda_{\overline{\text{MS}}}$ for the pure gauge theories and for the theories with 2 fundamental fermions. For completeness, we derive an expression (see eq. (5.12)) for the ratio $\Lambda_{\text{SF}}/\Lambda_{\overline{\text{MS}}}$ as a function of N, N_f and the representation R, which might be useful also for future BSM studies using the SF.

The Λ parameter is a renormalization group invariant and scheme dependent quantity given by (in a generic scheme X)

$$\Lambda_X = \mu \left(b_0 g_X^2\right)^{-\frac{b_1}{(2b_0^2)}} e^{-\frac{1}{(2b_0 g_X^2)}} \exp\left\{-\int_0^{g_X} dx \left[\frac{1}{\beta_X(x)} + \frac{1}{b_0 x^3} - \frac{b_1}{b_0^2 x}\right]\right\}. \tag{5.1}$$

It is a dimensionfull scale dynamically generated by the theory.

In subsection 4.2.2 we have performed the computation of the SF coupling[8] $\overline{g}_{\text{SF}}$ in the Schrödinger Functional scheme to one loop order in perturbation theory, i.e. we have calculated the renormalized coupling as an expansion in terms of the bare coupling g_0

$$\overline{g}^2_{\text{SF}}(L) = g_0^2 + p_1(L/a) g_0^4 + O(g_0^6), \tag{5.2}$$

where, after doing a continuum extrapolation,

$$p_1(L/a) = r_0 + 2b_0 \ln(L/a). \tag{5.3}$$

To be able to compare the results at different values of N, we are interested in a relation between $\alpha_{\text{SF}} = \overline{g}^2_{\text{SF}}/4\pi$ and some scheme where N is only a parameter. For that we choose the usual $\overline{\text{MS}}$ scheme, defined at infinite volume and at high energies. The relation between the running coupling in the two schemes can be written as an expansion

$$\alpha_{\overline{\text{MS}}}(s\mu) = \alpha_{\text{SF}}(\mu) + c_1(s)\alpha_{\text{SF}}(\mu)^2 + c_2(s)\alpha_{\text{SF}}(\mu)^3 + O(\alpha^4_{\text{SF}}), \tag{5.4}$$

where s is a scale parameter and $c_i(s)$ are the coefficients relating the couplings in the two schemes at each order in perturbation theory.

[8] In the following we write explicitly a subindex with the coupling to indicate the scheme.

JHEP11(2014)074

The relation between the Λ parameter in the SF and $\overline{\text{MS}}$ scheme is given by

$$\frac{\Lambda_{\text{SF}}}{\Lambda_{\overline{\text{MS}}}} = \exp\left\{-\frac{c_1(1)}{(8\pi b_0)}\right\}, \tag{5.5}$$

where $c_1(1)$ is the coefficient of the 1-loop relation (5.4). Note that eq. (5.5) is an exact relation even though it depends on the 1-loop coefficient relating the couplings in two different schemes.

For determining the coefficient $c_1(s)$ in eq. (5.4), we first use the known relation between $\alpha_{\overline{\text{MS}}}$ in the $\overline{\text{MS}}$ and the bare coupling α_0 [17, 30, 33, 40], which at 1-loop is given by

$$\alpha_{\overline{\text{MS}}}(s/a) = \alpha_0 + d_1(s)\alpha_0^2 + O(\alpha_0^3). \tag{5.6}$$

The 1-loop coefficient $d_1(s)$ is given for generic N and fermionic representation R by

$$d_1(s) = d_{1,0} + N_f d_{1,1} - 8\pi b_0 \ln(s), \tag{5.7}$$

where

$$d_{1,0} = -\frac{\pi}{2N} + k_1 N \qquad \text{and} \qquad d_{1,1} = \widetilde{K}_1 T_R. \tag{5.8}$$

The coefficient k_1 of the gauge part is taken from [17, 30, 33] and reads

$$k_1 = 2.135730074078457(2). \tag{5.9}$$

The coefficient $\widetilde{K}_1$ is a representation independent function of the tree level coefficient $c_{\text{sw}}^{(0)}$ given by

$$\widetilde{K}_1(c_{\text{sw}}^{(0)}) = -0.1682888(2) + 0.126838(2)c_{\text{sw}}^{(0)} - 0.750048(2)(c_{\text{sw}}^{(0)})^2. \tag{5.10}$$

It was calculated in [41–43] for the fundamental representation and extended to arbitrary representations in [40].

Combining eqs. (5.2) and (2.17) we obtain the coefficient for the relation (5.4), i.e.

$$c_1(s) = d_{1,0} + N_f d_{1,1} - 4\pi(r_{0,0} + N_f r_{0,1}) - 8\pi b_0 \ln(s), \tag{5.11}$$

with $r_{0,i}$ being the continuum coefficients in the series (4.1).

Knowing this, the relation between Λ parameters in eq. (5.5) can be given as a function of the parameters N, N_f and T_R and of the coefficients $r_{0,i}$

$$\frac{\Lambda_{\text{SF}}}{\Lambda_{\overline{\text{MS}}}} = \exp\left\{\frac{3\pi^2/N - 6\pi(k_1 N + \widetilde{K}_1 T_R N_f) + 24\pi^2(r_{0,0} + N_f r_{0,1})}{11N - 4T_R N_f}\right\}. \tag{5.12}$$

Finally, in table 5 we collect the values of the ratio of Λ parameters for the schemes studied in this work and for the pure gauge theory ($N_f = 0$) and for 2 flavors of fundamental fermions.[9] Ratios of lambda parameters for 2 index representations can be recovered using eq. (5.12) and the corresponding coefficients from table 3.

[9] Note that different choices of boundary phases or θ parameter correspond to different choices of renormalization scheme and will hence lead to different values for the ratio $\Lambda_{\text{SF}}/\Lambda_{\overline{\text{MS}}}$.

JHEP11(2014)074

N	$\Lambda_{\rm SF}/\Lambda_{\overline{\rm MS}}\big\vert_{N_f=0}$	$\Lambda_{\rm SF}/\Lambda_{\overline{\rm MS}}\big\vert_{N_f=2}$
2	0.44566597(1)	0.779492(3)
3	0.48811256(1)	0.699183(2)
4	0.503112529(5)	0.654811(1)
5	0.521195149(4)	0.6426328(9)
6	0.539386422(6)	0.6422183(8)
7	0.556975178(5)	0.6470850(6)
8	0.573795805(3)	0.6545895(6)
9	0.589843423(7)	0.6634798(5)
10	0.60516382(7)	0.6731035(4)
11	0.61981639(6)	0.6830971(4)
12	0.63385977(6)	0.6932473(3)

Table 5. Ratios between Λ parameters in the SF and $\overline{\rm MS}$ schemes, for the pure gauge theory and for 2 flavors of fundamental fermions.

6 Conclusions

We have studied the Schrödinger functional boundary conditions and the perturbative $\mathcal{O}(a)$ improvement for SU(N) gauge theories with general N. The improvement coefficient $c_t^{(1,0)}$ is obtained also for all values of N. Additionally we provide the matching between the SF and $\overline{\rm MS}$ schemes for a wide range of theories including fermions in various representations. This enables a precision study of the coupling and the determination of $\Lambda_{\overline{\rm MS}}$ in the large N limit.

The fermionic twisting angle θ is also studied and we found out that the value $\theta = \pi/2$ is a good compromise between the simulation speed and the minimization of the $\mathcal{O}(a^2)$ lattice artifacts in the perturbative 1-loop lattice step scaling function.

Acknowledgments

This work was supported by the Danish National Research Foundation DNRF:90 grant and by a Lundbeck Foundation Fellowship grant. TK is also funded by the Danish Institute for Advanced Study. PV gratefully acknowledges support by the EU under grant agreement number PITN-GA-2009-238353 (ITN STRONGnet) and by the INFN progetto premiale "SUMA". We thank Biagio Lucini and Stefan Sint for useful discussions.

A Details of the perturbative calculations

In this appendix we provide details on the calculation for an arbitrary group SU(N) of the ghost and gauge contributions $h_0(L/a)$ and $h_1(L/a)$ to the 1 loop coupling (see eqs. (2.20) and (2.21)). All the calculations are presented in a general framework. The specific values

JHEP11(2014)074

of different variables with our choice of background field and basis for SU(N) generators are shown in appendix B. In the following we will work in lattice units i.e. the lattice spacing $a = 1$. Additionally repeated Latin indices $a, b, c, \ldots$ are *not* summed over and repeated Greek indices $\alpha, \beta, \gamma, \ldots$ are always summed over unless otherwise stated in the formula. Latin indices run from $1, 2, 3$ and Greek ones from $0, 1, 2, 3$.

The operators we are interested in are defined as

$$\Delta_0 \omega(x) = -D^*_\mu D_\mu \omega(x), \tag{A.1}$$

$$\begin{aligned}\Delta_1 q_\mu(x) = &-\lambda_0 D_\mu D^*_\nu q_\nu(x) + \sum_{\nu \neq \mu} \big\{ \cosh(a^2 G_{\mu\nu}) \star [-D^*_\nu D_\nu q_\mu(x) + D^*_\nu D_\mu q_\nu(x)] \\ &- a^{-2} \sinh(a^2 G_{\mu\nu}) \star [2 q_\nu(x) + a(D^*_\nu + D_\nu) q_\mu(x) + a^2 D^*_\nu D_\mu q_\nu(x)] \big\}\,,\end{aligned} \tag{A.2}$$

$$\Delta_2 \psi(x) = \left[(D_{\mathrm{WD}} + m_0)\, \gamma_5 \right]^2 \psi(x). \tag{A.3}$$

There is no summation over μ in the r.h.s. of the eq. (A.2). The star product in eq. (A.2) which maps an $N \times N$ matrix M and an SU(N) matrix X to an SU(N) matrix is defined as

$$M \star X = \left(MX + XM^\dagger \right)/2 - \mathrm{Tr}\left(MX + XM^\dagger \right)/(2N). \tag{A.4}$$

In eq. (A.3) the operator D_{WD} is the same as in eq. (2.8) with $c_{\mathrm{sw}} = 1$.

The first step is to find a suitable basis for the SU(N) generators. This is a basis that is invariant under the star product defined in eq. (A.4). In practice we want to find generators X^a that satisfy

$$\begin{aligned}\cosh G_{0k} \star X^a &= \chi^c_a X^a, \\ \sinh G_{0k} \star X^a &= \chi^s_a X^a,\end{aligned} \tag{A.5}$$

with arbitrary coefficients χ^c_a and χ^s_a. The hyperbolic sine and cosine of the non-zero elements of the field strength tensor are

$$\cosh G_{0k} = \cos\left[(C'_k - C_k)/L \right], \qquad \sinh G_{0k} = i \sin\left[(C'_k - C_k)/L \right]. \tag{A.6}$$

A basis that satisfies eq. (A.5) for the non-diagonal generators are the ladder operators defined as

$$\left(X^{a(j,k)} \right)_{nm} = -i/2 \delta_{jn} \delta_{km}, \tag{A.7}$$

where n and m are the matrix indices and $a(j,k)$ is the color index. The properties of $a(j,k)$ are given in table 6. The generators X^a are normalized as $\mathrm{Tr}\left[X^a X^b \right] = -\frac{1}{2}\delta^{a,b}$. The diagonal generators can be chosen in any way that satisfies eq. (A.5).

The boundary conditions generate a background field $V_\mu(x)$ defined in eqs. (3.3), (3.4) and (3.5) which enters the covariant derivatives

$$\begin{aligned}D_\mu q(x) &= \left[V_\mu(x) q(x + \hat{\mu}) V^{-1}_\mu(x) - q(x) \right], \\ D^*_\mu q(x) &= \left[q(x) - V^{-1}_\mu(x - \hat{\mu}) q(x - \hat{\mu}) V_\mu(x - \hat{\mu}) \right],\end{aligned} \tag{A.8}$$

JHEP11(2014)074

$a(j,k)$	Range in a	Range in j	Range in k
$(N-j/2)(j-1)+(k-j)$	$1,\ldots,N(N-1)/2$	$1,\ldots,N-1$	$j+1,\ldots,N$
$(j-1)(j/2-1)+k+N(N-1)/2$	$N(N-1)/2+1,\ldots,N^2-N$	$2,\ldots,N$	$1,\ldots,j-1$

Table 6. The values of the color index $a(j,k)$ as a function of the dummy indices j and k. When $1 \leq a \leq (N^2-N)/2$ the generators X^a have a non-zero element in the upper and for $(N^2-N)/2 < a \leq N^2-N$ in the lower triangle.

and through them to the operators Δ_s. The next step is to calculate the covariant derivatives with the background field $V_\mu(x)$ when $q(x) = q_a(x)X^a$ is proportional to a generator X^a. The covariant derivatives can then be written in a general form

$$D_\mu q(x) = \begin{cases} [q_a(x+\hat{\mu}) - q_a(x)]\, X^a, & \text{if } \mu = 0, \\ [\exp(if_a)q_a(x+\hat{\mu}) + q_a(x)]\, X^a, & \text{if } \mu > 0, \end{cases} \tag{A.9}$$

$$D^*_\mu q(x) = \begin{cases} [q_a(x) - q_a(x-\hat{\mu})]\, X^a, & \text{if } \mu = 0, \\ [q_a(x) - \exp(-if_a)q_a(x-\hat{\mu})]\, X^a, & \text{if } \mu > 0, \end{cases} \tag{A.10}$$

where

$$[B_k(x), X^a] = if_a(t)X^a, \tag{A.11}$$

and t is the time component of the four vector $x = (t, \boldsymbol{x})$. The operators Δ_0 and Δ_1 can now be decomposed to color subspaces according to the basis selected. The operators are also invariant under spatial translations and thus the determinants can be written as

$$\det \Delta_s = \prod_a \prod_p \det \Delta_s|_{(p,a)}, \qquad s = 0, 1, \tag{A.12}$$

where

$$p = 2\pi n/L, \qquad n_k \in \mathbb{Z}, \qquad -L/2 < n_k \leq L/2, \tag{A.13}$$

is the three momentum.

Next we will show how one can calculate the determinant of operators Δ_s. In [1] it has been shown that for an operator Δ that satisfies

$$\Delta\psi(t) = A(t)\psi(t+1) + B(t)\psi(t) + C(t)\psi(t-1), \tag{A.14}$$

for matrices A, B and C and an eigenvalue equation

$$\begin{cases} (\Delta - \xi)\psi(t) = 0, & t > 0, \\ \psi(0) = \psi(L) = 0, \end{cases} \tag{A.15}$$

there exists a matrix $M(\xi)$ such that

$$\psi(L) = M(\xi)\psi(1) = 0. \tag{A.16}$$

The determinant of Δ is then given by

$$\det \Delta = \det M(0) \prod_{t=1}^{L-1} \det[-A(t)]. \tag{A.17}$$

We will next use these properties of the Δ_s operators.

Since the operator Δ_0 is invariant under spatial translations and constant diagonal gauge transformations its eigenfunctions are of the form

$$\omega_a(x) = \psi_a(t) e^{ipx} X^a. \tag{A.18}$$

Operating with Δ_0 on $\omega_a(x)$ we get

$$\Delta_0 \omega_a(x) = \left[A\psi_a(t+1) + B_a(t)\psi_a(t) + C\psi_a(t-1)\right] e^{ipx} X^a, \tag{A.19}$$

with $A = C = -1$ and

$$B_a(t) = 8 - 2\sum_{k=1}^{3} \cos\left[p_k + f_a(t)\right]. \tag{A.20}$$

Clearly the operator Δ_0 is similar to the operator in eq. (A.14) and thus the strategy shown can be used. Using the eq. (A.15) with $\xi = 0$ i.e.

$$\Delta_0 \psi_a(t) = 0, \qquad 0 \le t < L \tag{A.21}$$

we get a recursion relation for $\psi_a(t)$ with initial values $\psi_a(0) = 0$, $\psi_a(1) = 1$ which is

$$\psi_a(2) = B_a(1), \tag{A.22}$$

$$\psi_a(t+1) = B_a(t)\psi_a(t) - \psi_a(t-1), \qquad t \ge 2. \tag{A.23}$$

According to eq. (A.17) the determinant is then

$$\det \Delta_0|_{(p,a)} = \psi_a(L). \tag{A.24}$$

We will then move on to the more challenging case of Δ_1. The eigenfunctions of the operator Δ_1 have the general form

$$q^a_\mu(x) = R^a_{\mu\nu}(t)\psi^a_\nu(t) e^{ipx} X^a, \tag{A.25}$$

where normalization[10] matrix $R^a_{\mu\nu}(t)$ is a diagonal 4×4 matrix with

$$R^a_{00}(t) = -i, \qquad R^a_{kk}(t) = e^{i(p_k + f_a(t))/2}, \qquad k = 1, 2, 3. \tag{A.26}$$

Again we can operate with Δ_1 on the eigenfunction eq. (A.25) which yields

$$\Delta_1 q^a_\mu(x) = R^a_{\mu\nu}(t)\left[A^a_{\nu\rho}(t)\psi^a_\rho(t+1) + B^a_{\nu\rho}(t)\psi^a_\rho(t) + C^a_{\nu\rho}(t)\psi^a_\rho(t-1)\right] e^{ipx} X^a, \tag{A.27}$$

[10] Adding $R^a_{\mu\nu}$ ensures that the matrices $A^a_{\mu\nu}(t)$, $B^a_{\mu\nu}(t)$ and $C^a_{\mu\nu}(t)$ in the recursion relation are real.

JHEP11(2014)074

where the matrices $A^a_{\mu\nu}(t)$, $B^a_{\mu\nu}(t)$ and $C^a_{\mu\nu}(t)$ are

$$A^a_{\mu\nu}(t) = \begin{cases} A^a_{00}(t) &= -\lambda_0, \\ A^a_{kl}(t) &= -N^a \delta_{k,l}, \\ A^a_{0k}(t) &= \lambda_0 s^a_k(t+1) - N^a s^a_k(t), \\ A^a_{k0}(t) &= 0, \end{cases}$$

$$B^a_{\mu\nu}(t) = \begin{cases} B^a_{00}(t) &= 2\lambda_0 + \sum_{k=1}^3 s^a_k(t)\left(\chi^c_a s^a_k(t) - i\chi^s_a c^a_k(t)\right), \\ B^a_{kl}(t) &= (\lambda_0 - 1) s^a_k(t) s^a_l(t) + \delta_{k,l}\left(2\chi^c_a + \sum_{n=1}^3 (s^a_n(t))^2\right), \\ B^a_{0k}(t) &= \chi^c_a s^a_k(t) - i\chi^s_a c^a_k(t) - \lambda_0 s^a_k(t), \\ B^a_{k0}(t) &= B^a_{0k}(t), \end{cases} \tag{A.28}$$

$$C^a_{\mu\nu}(t) = A^a_{\nu\mu}(t-1).$$

We have used the following short handed notation

$$c^a_k(t) = 2\cos\left[(p_k + f_a(t))/2\right], \tag{A.29}$$

$$s^a_k(t) = 2\cos\left[(p_k + f_a(t))/2\right], \tag{A.30}$$

$$N^a = (\chi^c_a - \chi^s_a)\exp\left[i(f_a(t+1) - f_a(t))/2\right]. \tag{A.31}$$

The operator Δ_1 is also similar to the case in eq. (A.14) and the same strategy can again be exploited. Additionally the boundary conditions of $\psi^a_\mu(t)$ in eq. (A.27) are

$$\psi^a_0(-1) = \partial^*\psi^a_0(L) = \psi^a_k(0) = \psi^a_k(L) = 0, \qquad \boldsymbol{p} = 0 \bigwedge a > N^2 - N, \tag{A.32}$$

$$\partial^*\psi^a_0(0) = \partial^*\psi^a_0(L) = \psi^a_k(0) = \psi^a_k(L) = 0, \qquad \text{else.} \tag{A.33}$$

With this we can first calculate the determinant of Δ_1 in the more general case where the boundary conditions are given by eq. (A.33). Setting $\xi = 0$ in eq. (A.15) we get

$$\Delta_1\psi^a_0(t) = 0, \qquad 0 \le t < L, \tag{A.34}$$

$$\Delta_1\psi^a_k(t) = 0, \qquad 0 < t < L. \tag{A.35}$$

With the help of these equations we find $F^a_{\mu\nu}(t)$ which has the property

$$\psi^a_\mu(t) = F^a_{\mu\nu}(t) v^a_\nu, \tag{A.36}$$

where

$$v^a_\nu = \begin{pmatrix} \psi^a_0(0) \\ \psi^a_k(1) \end{pmatrix}, \tag{A.37}$$

JHEP11(2014)074

are the first nonzero components of $\psi^a_\mu(t)$. The matrix $F^a_{\mu\nu}(t)$ is

$$F^a_{\mu\nu}(1) = \begin{cases} -\left[B^a_{00}(0) + C^a_{00}(0)\right]/A^a_{00}(0), & \mu = \nu = 0, \\ -A^a_{0k}(0)/A^a_{00}(0), & \mu = 0 \bigwedge \nu = k \neq 0, \\ 0, & \mu \neq 0 \bigwedge \nu = 0, \\ \delta_{k,l}, & \mu = k \neq 0 \bigwedge \nu = l \neq 0, \end{cases} \tag{A.38}$$

$$F^a_{\mu\nu}(2) = -\left(A^a_{\mu\rho}(1)\right)^{-1}\left[B^a_{\rho\sigma}(1)F^a_{\sigma\nu}(1) + C^a_{\rho\sigma}(1)P_{\sigma\nu}\right],$$

$$F^a_{\mu\nu}(t+1) = -\left(A^a_{\mu\rho}(t)\right)^{-1}\left[B^a_{\rho\sigma}(t)F^a_{\sigma\nu}(t) + C^a_{\rho\sigma}(t)F^a_{\sigma\nu}(t-1)\right], \qquad t \geq 2,$$

where the projection operator $P_{\mu\nu}$ is

$$P_{\mu\nu} = \begin{cases} 1, & \mu = \nu = 0, \\ 0, & \text{else.} \end{cases} \tag{A.39}$$

With $F^a_{\mu\nu}(t)$ we will be able to construct a matrix $M^a_{\mu\nu}$ that couples v^a_μ from eq. (A.37) and the boundary condition eq. (A.33) at $t = L$

$$\begin{pmatrix} \partial^* \psi^a_0(L) \\ \psi^a_k(L) \end{pmatrix} = M^a_{\mu\nu} v^a_\nu. \tag{A.40}$$

This matrix $M^a_{\mu\nu}$ turns out to be

$$M^a_{\mu\nu} = F^a_{\mu\nu}(L) - P_{\mu\rho}F^a_{\rho\nu}(L-1), \tag{A.41}$$

and the determinant of Δ_1 in this subspace according to eq. (A.17) is

$$\det \Delta_1|_{(p,a)} = \det\left[M^a_{\mu\nu}\lambda_0^L (N^a)^{3(L-1)}\right]. \tag{A.42}$$

We can then move on to the case of Δ_1 where $a > N^2 - N$ i.e. for diagonal generators X^a and when $\boldsymbol{p} = 0$. In this case the boundary conditions are given by eq. (A.32) and $\psi^a_0(t)$ and $\psi^a_k(t)$ components decouple since the matrices $A^a_{\mu\nu}(t)$, $B^a_{\mu\nu}(t)$ and $C^a_{\mu\nu}(t)$ are diagonal

$$A^a_{00}(t) = -\lambda_0, \tag{A.43}$$

$$A^a_{kk}(t) = -\chi^c_a, \qquad k = 1,2,3, \tag{A.44}$$

$$A^a_{\mu\nu}(t) = C^a_{\mu\nu}(t) = 1/2 B^a_{\mu\nu}(t). \tag{A.45}$$

Again using the eq. (A.34) and eq. (A.35) with the boundary conditions (A.32) we find that

$$\psi^a_0(L) = (L+1)\psi^a_0(0), \qquad \psi^a_k(L) = L\psi^a_k(1), \tag{A.46}$$

and then we can write down the matrix M that couples the first nonzero components of $\psi^a_\mu(t)$ and the boundary condition (A.32) at $t = L$ as in eq. (A.40). Now the matrix M is diagonal with entries

$$M_{00} = 1, \qquad M_{kk} = L, \qquad k = 1,2,3. \tag{A.47}$$

JHEP11(2014)074

According to the eq. (A.17) the contribution to the determinant of Δ_1 is then

$$\det \Delta_1|_{(p=0,a>N^2-N)} = \lambda_0^L L^3 (\chi_a^c)^{3(L-1)}. \tag{A.48}$$

Now we are ready to present the value of the pure gauge part of the 1-loop coefficient $p_{1,0}(L/a)$ in the SF coupling which is

$$\begin{aligned} p_{1,0}(L/a) &= h_0(L/a) - 1/2 h_1(L/a) \\ &= \frac{1}{\kappa} \sum_{p,a,s} \frac{\partial}{\partial \eta} \left[\ln \det \Delta_0|_{(p,a)} - 1/2 \ln \det \Delta_1|_{(p,a)} \right] \\ &= \frac{1}{\kappa} \left\{ \sum_{a=1}^{N^2-N} \sum_p \left[\frac{\psi_a'(L)}{\psi_a(L)} - \frac{3(L-1)}{2} \frac{(N^a)'}{N^a} - \frac{1}{2} M^{(-1)}_{\mu\nu} M'_{\nu\mu} \right] \right. \\ &\quad \left. - \frac{1}{2} \sum_{a=N^2-N+1}^{N^2-1} \left[3(L-1) \frac{(\chi_a^c)'}{\chi_a^c} + \sum_{p \neq 0} \left(3(L-1) \frac{(N^a)'}{N^a} + M^{(-1)}_{\mu\nu} M'_{\nu\mu} \right) \right] \right\}, \end{aligned} \tag{A.49}$$

where prime indicates partial derivative w.r.t. the parameter η, $M^{(-1)}_{\mu\nu}$ is the inverse matrix of $M_{\mu\nu}$ and the normalization κ is defined in eq. (2.13).

B Chosen basis for the diagonal generators and the values of the coefficients which depend on the background field

In appendix A we showed how the 1-loop coupling can be calculated for a generic background field and basis of generators. In here we will specify the basis that we have selected as well as the values of the coefficients χ_a^c, χ_a^s and $f_a(t)$.

We have chosen a basis given by

$$X_{kk}^{N^2-N+b} = \frac{i}{\sqrt{2b(b+1)}} \left[-b\delta_{b+2,k} + \sum_{j=1}^{b} \delta_{j+1,k} \right], \qquad (N > 3), \tag{B.1}$$

$$X_{kk}^{N^2-2} = i/2(\delta_{k,1} - \delta_{k,N}), \tag{B.2}$$

$$X_{kk}^{N^2-1} = \frac{i}{\sqrt{N(N-2)}} \left[-(N-2)(\delta_{k,1} + \delta_{k,N}) + \sum_{j=2}^{N-1} \delta_{j,k} \right], \tag{B.3}$$

for the diagonal generators of SU(N), and by eq. (A.7) for the non diagonal ones. With this choice the coefficients χ_a^c and χ_a^s from eq. (A.5) are

$$\chi^c_{a(i,j)} = \begin{cases} 1/2 \left[\cos\zeta(i) + \cos\zeta(j) \right], & 1 \leq a(i,j) \leq N^2 - N, \\ 0, & a(i,j) > N^2 - N, \end{cases} \tag{B.4}$$

$$\chi^s_{a(i,j)} = \begin{cases} 1/2 \left[\sin\zeta(i) - \sin\zeta(j) \right], & 1 \leq a(i,j) \leq N^2 - N \\ 0, & a(i,j) > N^2 - N. \end{cases} \tag{B.5}$$

JHEP11(2014)074

where

$$\zeta(i) = \frac{2\eta}{L^2}\left(\delta_{1,i} + \delta_{N,i} - \frac{2}{N-2}\sum_{k=2}^{N-1}\delta_{k,i}\right) + \frac{\pi}{NL^2}\left((N-2)(\delta_{1,i}+\delta_{N,i}) - 2\sum_{k=2}^{N-1}\delta_{k,i}\right). \tag{B.6}$$

The coefficients $f_a(t)$ are[11]

$$\begin{aligned} f_{a(i,j)}(t) = {} & \frac{\pi}{2LN}\sum_{b=2}^{N-3}\left[\sum_{r=2}^{b+1}(\delta_{i,r}-\delta_{j,r}) - b\,(\delta_{i,b+2}-\delta_{j,b+2})\right] \\ & + \frac{(L-2t)(2\eta N + \pi(N-2))}{L^2(N-2)N}\left[\sum_{r=2}^{N-1}(\delta_{r,i}-\delta_{r,j}) + \frac{(N-2)}{2}(\delta_{N,j}-\delta_{1,i})\right] \\ & + \frac{\pi}{2LN}\left[\delta_{i,2}-\delta_{i,3}-\delta_{j,2}+\delta_{j,3}+(2N-1)\,(\delta_{1,i}+\delta_{N,j})\right], \end{aligned} \tag{B.7}$$

for $a \leq N^2 - N$ and $f_a = 0$ for $a > N^2 - N$.

Additionally the normalization in eq. (2.13) depends on the chosen background field. For our choice it is

$$\kappa = 24L^2\left\{\sin\left[\left(\left(1-\frac{2}{N}\right)\pi + 2\eta\right)/L^2\right] + \sin\left[2\left(\frac{\pi}{N} + \frac{2\eta}{N-2}\right)/L^2\right]\right\}. \tag{B.8}$$

References

[1] M. Lüscher, R. Narayanan, P. Weisz and U. Wolff, *The Schrödinger functional: A Renormalizable probe for nonAbelian gauge theories*, *Nucl. Phys.* **B 384** (1992) 168 [hep-lat/9207009] [INSPIRE].

[2] M. Lüscher, R. Sommer, U. Wolff and P. Weisz, *Computation of the running coupling in the* SU(2) *Yang-Mills theory*, *Nucl. Phys.* **B 389** (1993) 247 [hep-lat/9207010] [INSPIRE].

[3] M. Lüscher, R. Sommer, P. Weisz and U. Wolff, *A Precise determination of the running coupling in the* SU(3) *Yang-Mills theory*, *Nucl. Phys.* **B 413** (1994) 481 [hep-lat/9309005] [INSPIRE].

[4] ALPHA collaboration, M. Della Morte et al., *Computation of the strong coupling in QCD with two dynamical flavors*, *Nucl. Phys.* **B 713** (2005) 378 [hep-lat/0411025] [INSPIRE].

[5] B. Lucini and G. Moraitis, *The Running of the coupling in* SU(N) *pure gauge theories*, *Phys. Lett.* **B 668** (2008) 226 [arXiv:0805.2913] [INSPIRE].

[6] T. Appelquist, G.T. Fleming and E.T. Neil, *Lattice study of the conformal window in QCD-like theories*, *Phys. Rev. Lett.* **100** (2008) 171607 [*Erratum ibid.* **102** (2009) 149902] [arXiv:0712.0609] [INSPIRE].

[11] This expression holds for $N \geq 3$. In the case when $3 \leq N < 5$ it must be noted that the sum over b does not exist and thus the first term does not contribute.

JHEP11(2014)074

[7] A.J. Hietanen, K. Rummukainen and K. Tuominen, *Evolution of the coupling constant in* SU(2) *lattice gauge theory with two adjoint fermions*, *Phys. Rev.* **D 80** (2009) 094504 [arXiv:0904.0864] [INSPIRE].

[8] T. Karavirta, J. Rantaharju, K. Rummukainen and K. Tuominen, *Determining the conformal window:* SU(2) *gauge theory with* $N_f = 4$, 6 *and* 10 *fermion flavours*, *JHEP* **05** (2012) 003 [arXiv:1111.4104] [INSPIRE].

[9] F. Bursa, L. Del Debbio, L. Keegan, C. Pica and T. Pickup, *Mass anomalous dimension in* SU(2) *with two adjoint fermions*, *Phys. Rev.* **D 81** (2010) 014505 [arXiv:0910.4535] [INSPIRE].

[10] F. Bursa, L. Del Debbio, L. Keegan, C. Pica and T. Pickup, *Mass anomalous dimension in* SU(2) *with six fundamental fermions*, *Phys. Lett.* **B 696** (2011) 374 [arXiv:1007.3067] [INSPIRE].

[11] T. DeGrand, Y. Shamir and B. Svetitsky, *Running coupling and mass anomalous dimension of* SU(3) *gauge theory with two flavors of symmetric-representation fermions*, *Phys. Rev.* **D 82** (2010) 054503 [arXiv:1006.0707] [INSPIRE].

[12] T. DeGrand, Y. Shamir and B. Svetitsky, SU(4) *lattice gauge theory with decuplet fermions: Schrödinger functional analysis*, *Phys. Rev.* **D 85** (2012) 074506 [arXiv:1202.2675] [INSPIRE].

[13] M. Hayakawa, K.-I. Ishikawa, Y. Osaki, S. Takeda, S. Uno and N. Yamada, *Running coupling constant of ten-flavor QCD with the Schrödinger functional method*, *Phys. Rev.* **D 83** (2011) 074509 [arXiv:1011.2577] [INSPIRE].

[14] U.M. Heller, *The Schrödinger functional running coupling with staggered fermions and its application to many flavor QCD*, *Nucl. Phys. Proc. Suppl.* **63** (1998) 248 [hep-lat/9709159] [INSPIRE].

[15] S. Sint and R. Sommer, *The Running coupling from the QCD Schrödinger functional: A One loop analysis*, *Nucl. Phys.* **B 465** (1996) 71 [hep-lat/9508012] [INSPIRE].

[16] M. Lüscher and P. Weisz, $O(a)$ *improvement of the axial current in lattice QCD to one loop order of perturbation theory*, *Nucl. Phys.* **B 479** (1996) 429 [hep-lat/9606016] [INSPIRE].

[17] M. Lüscher, S. Sint, R. Sommer and P. Weisz, *Chiral symmetry and* $O(a)$ *improvement in lattice QCD*, *Nucl. Phys.* **B 478** (1996) 365 [hep-lat/9605038] [INSPIRE].

[18] B. Sheikholeslami and R. Wohlert, *Improved Continuum Limit Lattice Action for QCD with Wilson Fermions*, *Nucl. Phys.* **B 259** (1985) 572 [INSPIRE].

[19] B. Lucini and M. Panero, SU(N) *gauge theories at large-*N, *Phys. Rept.* **526** (2013) 93 [arXiv:1210.4997] [INSPIRE].

[20] R. Narayanan and H. Neuberger, *Infinite N phase transitions in continuum Wilson loop operators*, *JHEP* **03** (2006) 064 [hep-th/0601210] [INSPIRE].

[21] M. Lüscher, *Properties and uses of the Wilson flow in lattice QCD*, *JHEP* **08** (2010) 071 [arXiv:1006.4518] [INSPIRE].

[22] M. Lüscher and P. Weisz, *Perturbative analysis of the gradient flow in non-abelian gauge theories*, *JHEP* **02** (2011) 051 [arXiv:1101.0963] [INSPIRE].

[23] A. Ramos, *The gradient flow in a twisted box*, PoS(Lattice 2013)053 [arXiv:1308.4558] [INSPIRE].

[24] P. Fritzsch and A. Ramos, *The gradient flow coupling in the Schrödinger Functional*, *JHEP* **10** (2013) 008 [arXiv:1301.4388] [INSPIRE].

JHEP11(2014)074

[25] A. Ramos, plenary talk in *Lattice 2014*.

[26] J. Rantaharju, *The Gradient Flow Coupling in Minimal Walking Technicolor*, PoS(Lattice 2013)084 [arXiv:1311.3719] [INSPIRE].

[27] R. Narayanan and H. Neuberger, *Large-N reduction in continuum*, *Phys. Rev. Lett.* **91** (2003) 081601 [hep-lat/0303023] [INSPIRE].

[28] F. Sannino and K. Tuominen, *Orientifold theory dynamics and symmetry breaking*, *Phys. Rev.* **D 71** (2005) 051901 [hep-ph/0405209] [INSPIRE].

[29] T. Karavirta, A. Hietanen and P. Vilaseca, *Schrödinger functional boundary conditions and improvement of the* SU(N) *pure gauge action for* $N > 3$, PoS(LATTICE 2013)328 [arXiv:1311.0405] [INSPIRE].

[30] S. Sint, *One loop renormalization of the QCD Schrödinger functional*, *Nucl. Phys.* **B 451** (1995) 416 [hep-lat/9504005] [INSPIRE].

[31] R. Wohlert, *Improved Continuum Limit Lattice Action For Quarks*, DESY87/069 [INSPIRE].

[32] T. Karavirta, A. Mykkanen, J. Rantaharju, K. Rummukainen and K. Tuominen, *Nonperturbative improvement of* SU(2) *lattice gauge theory with adjoint or fundamental flavors*, *JHEP* **06** (2011) 061 [arXiv:1101.0154] [INSPIRE].

[33] M. Lüscher, S. Sint, R. Sommer, P. Weisz and U. Wolff, *Nonperturbative* $O(a)$ *improvement of lattice QCD*, *Nucl. Phys.* **B 491** (1997) 323 [hep-lat/9609035] [INSPIRE].

[34] S. Sint and P. Vilaseca, *Lattice artefacts in the Schrödinger Functional coupling for strongly interacting theories*, PoS(LATTICE 2012)031 [arXiv:1211.0411] [INSPIRE].

[35] T. Karavirta, K. Tuominen and K. Rummukainen, *Perturbative Improvement of the Schrödinger Functional for Lattice Strong Dynamics*, *Phys. Rev.* **D 85** (2012) 054506 [arXiv:1201.1883] [INSPIRE].

[36] S. Sint and P. Vilaseca, *Perturbative lattice artefacts in the SF coupling for technicolor-inspired models*, PoS(LATTICE 2011)091 [arXiv:1111.2227] [INSPIRE].

[37] ALPHA collaboration, A. Bode, U. Wolff and P. Weisz, *Two loop computation of the Schrödinger functional in pure* SU(3) *lattice gauge theory*, *Nucl. Phys.* **B 540** (1999) 491 [hep-lat/9809175] [INSPIRE].

[38] ALPHA collaboration, A. Bode, P. Weisz and U. Wolff, *Two loop computation of the Schrödinger functional in lattice QCD*, *Nucl. Phys.* **B 576** (2000) 517 [*Erratum ibid.* **B 600** (2001) 453] [*Erratum ibid.* **B 608** (2001) 481] [hep-lat/9911018] [INSPIRE].

[39] M. Lüscher and P. Weisz, *Efficient Numerical Techniques for Perturbative Lattice Gauge Theory Computations*, *Nucl. Phys.* **B 266** (1986) 309 [INSPIRE].

[40] L. Del Debbio, M.T. Frandsen, H. Panagopoulos and F. Sannino, *Higher representations on the lattice: Perturbative studies*, *JHEP* **06** (2008) 007 [arXiv:0802.0891] [INSPIRE].

[41] P. Weisz, *On the Connection Between the* Λ *Parameters of Euclidean Lattice and Continuum QCD*, *Phys. Lett.* **B 100** (1981) 331 [INSPIRE].

[42] C. Christou, A. Feo, H. Panagopoulos and E. Vicari, *The Three loop* β*-function of* SU(N) *lattice gauge theories with Wilson fermions*, *Nucl. Phys.* **B 525** (1998) 387 [*Erratum ibid.* **B 608** (2001) 479] [hep-lat/9801007] [INSPIRE].

[43] S. Capitani and G. Rossi, *Deep inelastic scattering in improved lattice QCD. 1. The First moment of structure functions*, *Nucl. Phys.* **B 433** (1995) 351 [hep-lat/9401014] [INSPIRE].

JHEP11(2014)074